Spatially Modulated Antiferromagnetic Order in CoO/NiO Superlattices

J. A. Borchers,[1] M. J. Carey,[2] R. W. Erwin,[1] C. F. Majkrzak,[1] and A. E. Berkowitz[2]
[1] *National Institute of Standards and Technology, Gaithersburg, Maryland 20899*
[2] *Center for Magnetic Recording Research and Department of Physics, University of California at San Diego, La Jolla, California 92093-0401*
(Received 25 June 1992)

Neutron diffraction measurements confirm the presence of long-range antiferromagnetic order in superlattices of cobalt oxide and nickel oxide. A single transition temperature between the values for bulk CoO and NiO is evident for two samples with 36 Å periods as previously reported, but the separate Ni and Co order parameters in a 72 Å period superlattice approximate bulk behavior. In the latter sample the magnetic order remains coherent across ostensibly paramagnetic CoO interlayers above 400 K. Mean field analysis accounts for the layer thickness dependence of the ordering temperature.

PACS numbers: 75.25.+z, 75.50.Rr, 75.70.Fr

Because of recent advances in the controlled deposition of magnetic materials, the nature and strength of spin interactions can be examined systematically through the growth of thin films and superlattices. Most studies to date have focused on the transition [1] and rare-earth [2, 3] metals in which the coupling is long range. Systems with short-range interactions such as magnetic-semiconductor superlattices [4] are, in general, more straightforward because the exchange and anisotropy of the component materials are readily understood. For this reason, significant interest has developed in magnetic-insulator superlattices consisting of FeF_2/CoF_2 [5], Fe_3O_4/NiO [6], and NiO/CoO [7,8]. While the superlattices retain the antiferromagnetic or ferrimagnetic spin order of the constituents, the magnetic behavior near the phase transition reflects the influence of one material on the other.

In this Letter we report the magnetic structure of nickel-oxide/cobalt-oxide superlattices determined using neutron diffraction techniques. Even above the apparent CoO transition temperature in samples with thick CoO interlayers, antiferromagnetic order is coherent through several superlattice bilayers. Specifically, measurements of the spatially modulated order parameter in a 72 Å period sample suggest that the Ni and Co moments order at separate temperatures shifted from the T_N's for bulk CoO and NiO (291 and 520 K, respectively). The coherence of the spin structure monotonically decreases as the temperature is increased to 450 K, but remains greater than the width of a single bilayer though the Co moment is below the detection limit. In contrast, magnetic order develops simultaneously within the CoO and NiO layers for two superlattices with 36 Å periods. The measured transition temperatures, which fall between the Néel temperatures for bulk CoO and NiO, depend on the relative CoO and NiO layer thicknesses in a manner consistent with both Bando *et al.* observations [7] and the predictions of mean field theory.

CoO and NiO were chosen for this study because their magnetic properties contrast sharply while their similar structures allow for coherent growth. Both materials crystallize in the cubic NaCl structure with lattice parameters of 4.173 and 4.254 Å for NiO and CoO, respectively [9]. Below T_N these oxides order as collinear antiferromagnets with moments of $1.9\mu_B$ on the Ni sites and $3.8\mu_B$ on the Co sites. In NiO the spins are ferromagnetically aligned in sheets perpendicular to the [111] axis, with the moments alternating direction in adjacent planes. Though the in-plane anisotropy is small, the easy axis is parallel to $[1\bar{1}0]$ in annealed crystals [10]. Because of magnetostrictive effects, a slight rhombohedral distortion occurs below T_N with the [111] crystalline axis contracting by 0.12%. The magnetic structure for CoO is similar to that of NiO, except that the spins are tilted out of the (111) plane by an angle of 8° [11]. The large in-plane anisotropy further constrains the moments to lie in the $(1\bar{1}0)$ plane. A tetragonal deformation accompanies the magnetic transition—the [001] axis contracts by 1.2%.

The NiO/CoO superlattices considered in this study were prepared by reactive sputtering, but exhibit strong in-plane order [12] generally associated with controlled evaporation techniques. During growth the Co and Ni were sputtered from separate sources onto the (001) face of a 2″ diameter α-Al_2O_3 substrate in an argon (2.00 mTorr)/oxygen (0.09 mTorr) atmosphere. Complete details of the growth process are provided elsewhere [9]. X-ray diffraction measurements [12] show that the superlattices grow preferentially along the [111] direction. Fits of a superlattice model [12] to θ-2θ scans through the (111) Bragg reflection clearly demonstrate that diffusion at the interfaces extends over fewer than two atomic planes. The in-plane mosaic is roughly 3°–4°, and the samples are twinned in the growth plane [9].

Neutron diffraction studies were performed at the NIST reactor on two triple-axis spectrometers, BT-2 and

BT-9. An (002) PG monochromator was set to select neutrons with a wavelength of 2.35 Å, and a PG analyzer was set for zero energy transfer to reduce the inelastic background. Figure 1(b) shows a scan through the (111) structural reflections at 20 K for a superlattice comprising 100 bilayers with 43.1 Å of nickel oxide and 28.8 Å of cobalt oxide, denoted $[\mathrm{NiO(43\ Å)|CoO(29\ Å)}]_{100}$. Superlattice sidebands are separated from the central reflection at $K = 2.576\ \text{Å}^{-1}$ by $\Delta K = \pm 2\pi n/\Lambda$, with a superlattice period Λ of 71.9 Å. The integrated intensities of these peaks were fitted by a damped rectangle-wave model, which allows for atomic diffusion and strain gradients through the interfaces [3]. The fit suggests that the CoO lattice is stretched by 1.2% along the [111] direction to accommodate lattice matching in the growth plane, while the NiO lattice is essentially bulklike. Similar data analysis for $[\mathrm{NiO(21\ Å)|CoO(15\ Å)}]_{145}$ confirms that the epitaxial strain is confined to the CoO layers and that interlayer mixing is limited to two atomic planes at the NiO/CoO interfaces.

For $[\mathrm{NiO(43\ Å)|CoO(29\ Å)}]_{100}$ at 20 K, a strong magnetic reflection surrounded by superlattice sidebands is evident at $K = 1.290\ \text{Å}^{-1}$ in Fig. 1(a). The presence of these half-order peaks marks a doubling of the crystalline unit cell and suggests that ferromagnetic planes in the superlattice are antiparallel along the [111] axis as in the bulk-oxide components. Previous studies of similar NiO/CoO superlattices [7] imply that the antiferromagnetic order propagates along the growth axis through several bilayers. Indeed, the full width at half maximum (FWHM) of this magnetic reflection, obtained from a Gaussian fit, is $0.032\ \text{Å}^{-1}$ which gives a magnetic coherence length of 250 Å after deconvolution with the instrumental resolution.

The Ni and Co moment values were extracted from these data by comparing the integrated intensities of the $(\frac{1}{2}\frac{1}{2}\frac{1}{2})$ peaks to the (111) intensities within the framework of the damped-wave superlattice model [3]. (For these fits it is assumed that every Co or Ni atom has the same thermally averaged moment.) In the cubic structure, there are three equivalent [111] axes tilted 70.5° from the [111] growth direction which, due to twinning in the growth plane [9], give rise to six possible off-axis domains. Contrary to the Bando *et al.* report [7], only 25% of the nickel and cobalt moments lie in planes perpendicular to the growth axis for $[\mathrm{NiO(43\ Å)|CoO(29\ Å)}]_{100}$ at 20 K. Scans through the $(11\bar{1})$ and $(\frac{1}{2}\frac{1}{2}\frac{\bar{1}}{2})$ reflections for this sample show that the remaining 75% of the spins are spread among the six off-axis domains, which also extend through several bilayers. Assuming an equal distribution and combining the spin components in all seven domains, the Ni and Co moments obtained are $(2.0 \pm 0.3)\mu_B$ and $(4.4 \pm 0.7)\mu_B$, respectively, relative to $1.9\mu_B$ and $3.8\mu_B$ for the bulk oxides.

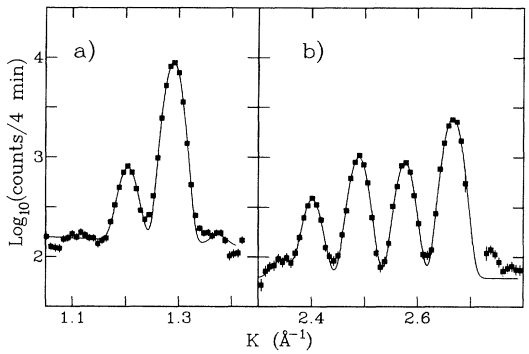

FIG. 1. (a) Neutron diffraction scan at 20 K along the (*lll*) direction through the $(\frac{1}{2}\frac{1}{2}\frac{1}{2})$ magnetic reflection for $[\mathrm{NiO(43\ Å)|CoO(29\ Å)}]_{100}$. The peaks have been fitted with Gaussians (solid line). (b) Neutron diffraction scan at 20 K through the (111) structural reflection for the same sample.

The intensity of the central magnetic reflection in Fig. 1(a) is roughly proportional to the square of the average sublattice moment through a single bilayer:

$$I \propto \left(\frac{N_{\mathrm{Ni}}\mu_{\mathrm{Ni}} + N_{\mathrm{Co}}\mu_{\mathrm{Co}}}{N_{\mathrm{Ni}} + N_{\mathrm{Co}}} \right)^2 , \tag{1}$$

where N_{Ni} and N_{Co} are the number of Ni and Co atomic planes per bilayer and μ_{Ni} and μ_{Co} are the Ni and Co moments. The temperature dependence of this peak intensity thus provides a measure of the "average" order parameter, which is plotted in Fig. 2(a) for the 72 Å and one of the 36 Å period superlattices, $[\mathrm{NiO(43\ Å)|CoO(29\ Å)}]_{100}$ and $[\mathrm{NiO(21\ Å)|CoO(15\ Å)}]_{145}$, respectively. The magnetic behavior exhibited by both 36 Å period samples ($[\mathrm{NiO(21\ Å)|CoO(15\ Å)}]_{145}$ and $[\mathrm{NiO(16\ Å)|CoO(20\ Å)}]_{150}$) is suggestive of a classical antiferromagnet, with the exception of a small tail evident near the ordering temperature. The nickel and cobalt moments in these samples order together at a single T_N of 410 K for the former sample and 383 K for the latter. These temperatures are approximately equal to the weighted average of the Néel temperatures for bulk NiO and CoO. Exchange anisotropy measurements on superlattices capped with permalloy overlayers [8] confirm that the ordering temperature scales with the relative thickness of the NiO and CoO layers. In addition, neutron diffraction studies by Bando and co-workers [7] on a similar series of NiO/CoO superlattices demonstrate that T_N exhibits this thickness dependence only when the superlattice period is small.

Contrasting with the data for the 36 Å period samples, the curvature of the order parameter for the 72 Å superlattice in Fig. 2(a) changes sharply above 320 K, with the emergence of a pronounced tail. The Ni and Co moments in the center of the layers, determined from fits of the neutron data by the damped-wave superlattice model, are plotted as a function of temperature in Fig. 3(a). Though the shape of the two curves is suggestive of bulk behavior, the apparent transition temperature for the central Co spins is roughly 80 K greater than

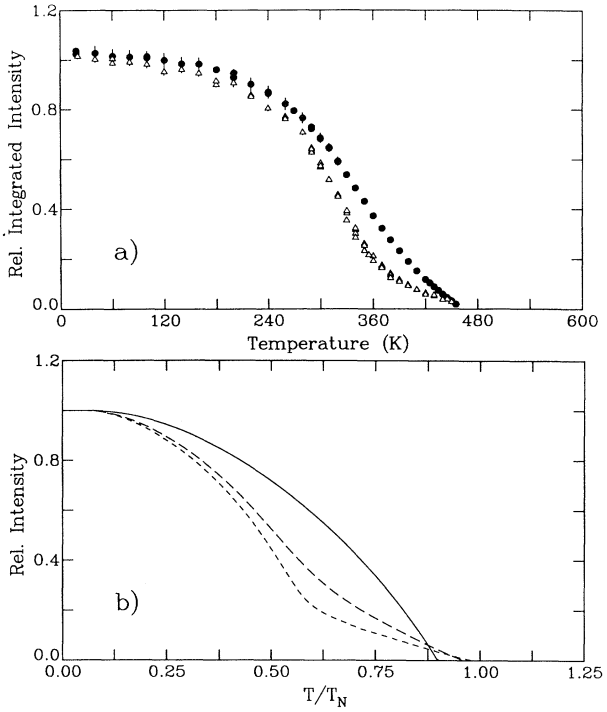

FIG. 2. (a) Temperature dependence of the integrated intensity of the central $(\frac{1}{2}\frac{1}{2}\frac{1}{2})$ magnetic peak for [NiO(21 Å)|CoO(15 Å)]$_{145}$ (dark circles) and [NiO(43 Å)|CoO(29 Å)]$_{100}$ (open triangles). (b) Mean field calculation of the relative intensity of the $(\frac{1}{2}\frac{1}{2}\frac{1}{2})$ peak as a function of temperature for NiO/CoO bilayers consisting of three (solid line), eight (long dashes), and fifteen (short dashes) atomic planes of both Ni and Co. The temperature is scaled by T_N for NiO.

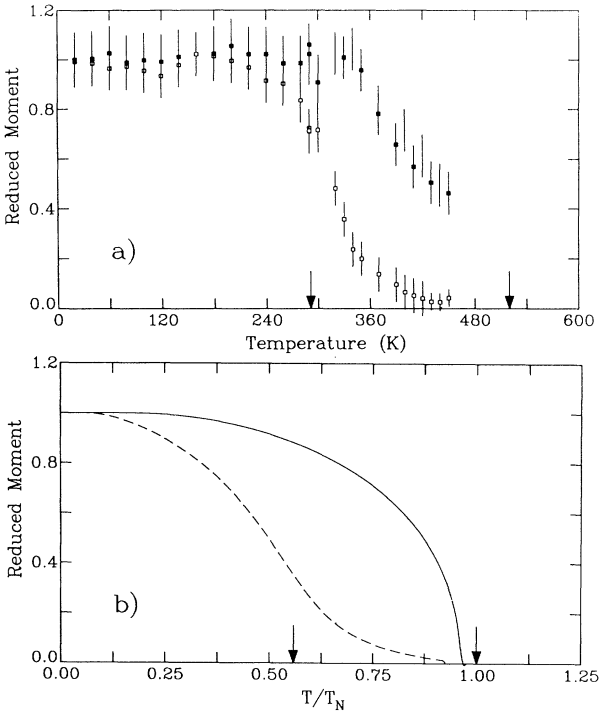

FIG. 3. (a) Temperature dependence of the Co (open squares) and Ni (dark squares) moments, in the center of the CoO and NiO layers, respectively, extracted from fits of the $(\frac{1}{2}\frac{1}{2}\frac{1}{2})$ and (111) diffraction data by the damped-wave superlattice model [3]. The moments have been scaled by their low-temperature saturation values. The T_N's of bulk NiO and CoO are marked by arrows. (b) Temperature dependence of the Ni (solid line) and Co (dashed line) moments calculated from the mean field model for a bilayer with $N_{\mathrm{NiO}} = N_{\mathrm{CoO}} = 8$. The ordering temperatures of the bulk components are designated by arrows.

$T_N = 291$ K for CoO, while T_N for the Ni moments is reduced from the 520 K bulk value. Similar shifts in the ordering temperatures have been reported for FeF_2/CoF_2 superlattices by Ramos *et al.* [5]. Above 400 K where the NiO is still ordered, the Co moment in the center of the CoO layers is zero within the error of the fits.

Above the inflection point in Fig. 2(a), the antiferromagnetic reflection begins to broaden as the Co moment value crosses below the Ni value. The magnetic coherence length for both 36 Å period samples, calculated from the FWHM of the $(\frac{1}{2}\frac{1}{2}\frac{1}{2})$ peak, remains constant at 250 Å with temperature, while the coherence for the 72 Å superlattice falls from 250 Å at 300 K to 170 Å at 450 K [13]. The gradual decrease of the coherence length reflects the loss of magnetic order in the CoO interlayers. Above 400 K, however, the Ni antiferromagnetic alignment persists through two superlattice bilayers, though the Co moments are effectively disordered. Even after cooling the sample from above T_N for NiO, long-range antiferromagnetic order spontaneously forms. Comparable measurements for a 97 Å period superlattice, [NiO(51 Å)|CoO(46 Å)]$_{25}$, indicate that 35–45 Å of CoO is required to confine the Ni spin order to a single NiO interlayer at temperatures approaching 520 K.

A simplified mean field approach provides a basis for understanding the magnetic order and its dependence upon layer thickness in these superlattices. In the model the magnetic structure through a single bilayer consisting of N_{NiO} planes of NiO and N_{CoO} planes of CoO is determined from a solution of mean field equations that include only nearest-neighbor exchange interactions. For the ith spin in the bilayer,

$$\langle S_i \rangle = \mathcal{B}_S \left(\frac{\mathcal{J}_i \langle S_{i-1} \rangle + \mathcal{J}_i \langle S_{i+1} \rangle}{k_B T} \right), \qquad (2)$$

where $\mathcal{B}_S$ is the Brillouin function. The effective spins $\langle S_{\mathrm{Ni}} \rangle$ and $\langle S_{\mathrm{Co}} \rangle$ are determined from the moments, $\mu = \sqrt{S(S+1)}$. It is assumed that the interlayer exchange parameters, $\mathcal{J}_{\mathrm{NiO}}$ and $\mathcal{J}_{\mathrm{CoO}}$, are negative and proportional to the Néel temperatures for bulk NiO and CoO and that $\mathcal{J}_i$ at the NiO/CoO interface equals the average of these two parameters. Figure 3(b) shows the

temperature dependence of the moments in the center of the NiO and CoO layers calculated for a bilayer with $N_{NiO} = N_{CoO} = 8$ ($\Lambda \approx 40$ Å). The qualitative behavior approximates the data for the 72 Å period sample, [NiO(43 Å)|CoO(29 Å)]$_{100}$ in Fig. 3(a), with the Ni and Co moments approaching zero at separate temperatures. As demonstrated by Wang and Mills [14], the model also predicts that just below the ordering temperature for NiO, the moment decays smoothly through the interfaces to near zero in the center of the CoO layers. We cannot extract the exact spatial variation of the moment through a single bilayer for [NiO(43 Å)|CoO(29 Å)]$_{100}$ because only three magnetic reflections can be resolved, but the shifting of the apparent ordering temperatures from the bulk values suggests that Co spins near the interface are polarized by exchange coupling to the Ni moments.

While the model indicates that only one, true phase transition exists for an ideal CoO/NiO superlattice, the temperature at which the Co sites develop measurable moments shifts toward T_N for bulk CoO as the CoO interlayer thickness is increased [14]. This result is exemplified by calculations of the average order parameter [Eq. (1)] for three different bilayers with $N_{NiO} = N_{CoO} = 3, 8,$ and 15 shown in Fig. 2(b). The similarity of the curve calculated for $N_{NiO} = N_{CoO} = 3$ and the data for [NiO(21 Å)|CoO(15 Å)]$_{145}$ in Fig. 2(a) confirm that the Ni and Co spins develop finite moments at a single T_N. Consistent with the diffraction measurements for [NiO(43 Å)|CoO(29 Å)]$_{100}$, a tail in the order parameter emerges at high temperatures as the superlattice period is increased.

Mean field calculations thus qualitatively describe the dependence of the ordering temperature on repeat distance. The accuracy of the molecular field description of these superlattices could possibly be improved by including magnetoelastic effects, important for the constituent oxides. In fact, neutron diffraction measurements of a 1000 Å CoO film, stretched 0.5% along the growth axis, indicate that antiferromagnetic order develops at a temperature 15 K greater than T_N for bulk [13]. By analogy, we expect that strain-induced enhancement of the CoO transition temperature is even greater in the epitaxial superlattices and may account for discrepancies between the spin-interaction length scales predicted by mean field and those observed experimentally.

In NiO/CoO superlattices the magnetic proximity effect gives rise to long-range spin alignment due to exchange coupling at the interfaces. Roughly 35 Å of CoO is sufficient to disrupt this coupling, as indicated by data for the superlattice with a 97 Å period. Though the reduction of the magnetic coherence length for the 72 Å superlattice follows the loss of magnetic order in the CoO interlayers at high temperatures, the spin structure propagates through several bilayers even above 400 K where the Co moment is zero with an uncertainty of $0.2\mu_B$. We can find no compelling evidence for the persistence of a small nonzero moment on the Co sites over a 100 deg temperature interval as expected from mean-field theory, but cannot refute its possible existence. Alternately this interlayer coupling may reflect exchange interactions of greater extent than previously determined [15]. In either case, this is the first reported observation of the propagation of antiferromagnetic spin order through an ostensibly paramagnetic interlayer in a superlattice system with short-range spin interactions.

The work at UCSD was supported through the National Science Foundation under Grant No. DMR-90-10908 and grants from the IBM Corporation and Storage Technology Corporation.

[1] L.M. Falicov, Daniel T. Pierce, S.D. Bader, R. Gronsky, Kristl B. Hathaway, Herbert J. Hopster, David N. Lambeth, S.S.P. Parkin, Gary Prinz, Myron Salamon, Ivan K. Schuller, and R.H. Victora, J. Mater. Res. **5**, 1299 (1990).

[2] C.F. Majkrzak, J. Kwo, M. Hong, Y. Yafet, Doon Gibbs, C.L. Chien, and J. Bohr, Adv. Phys. **40**, 99 (1991).

[3] J.A. Borchers, M.B. Salamon, R.W. Erwin, J.J. Rhyne, R.R. Du, and C.P. Flynn, Phys. Rev. B **43**, 3123 (1991); R.W. Erwin, J.J. Rhyne, M.B. Salamon, J. Borchers, Shantanu Sinha, R. Du, J.E. Cunningham, and C.P. Flynn, Phys. Rev. B **35**, 6808 (1987).

[4] N. Samarth, P. Klosowski, H. Luo, T.M. Giebultowicz, J.K. Furdyna, J.J. Rhyne, B.E. Larson, and N. Otsuka, Phys. Rev. B **44**, 4701 (1991).

[5] C.A. Ramos, D. Lederman, A.R. King, and V. Jaccarino, Phys. Rev. Lett. **65**, 2913 (1990).

[6] D.M. Lind, S.D. Berry, G. Chern, H. Mathias, and L.R. Testardi, Phys. Rev. B **45**, 1838 (1992); D.M. Lind, S.D. Berry, G. Chern, H. Mathias, and L.R. Testardi, J. Appl. Phys. **70**, 6218 (1991).

[7] Y. Bando, M. Takano, T. Terashima, and Z. Hiroi, in *Proceedings of the MRS International Meeting on Advanced Materials* (Materials Research Society, Pittsburgh, PA, 1989), Vol. 10, p. 83; M. Takano, T. Terashima, and Y. Bando, Appl. Phys. Lett. **51**, 205 (1987).

[8] M.J. Carey, A.E. Berkowitz, J.A. Borchers, and R.W. Erwin (unpublished).

[9] M.J. Carey, F.E. Spada, A.E. Berkowitz, W. Cao, and G. Thomas, J. Mater. Res. **6**, 2680 (1991).

[10] W.L. Roth, J. Appl. Phys. **31**, 2000 (1960).

[11] D. Herrmann-Ronzaud, P. Burlet, and J. Rossat-Mignod, J. Phys. C **11**, 2123 (1978).

[12] E.E. Fullerton, W. Cao, M.J. Carey, I.K. Schuller, G. Thomas, and A.E. Berkowitz, Appl. Phys. Lett. (to be published).

[13] J.A. Borchers, M.J. Carey, R.W. Erwin, A.E. Berkowitz, and C.F. Majkrzak, J. Appl. Phys. (to be published).

[14] R.W. Wang and D.L. Mills, Phys. Rev. B **46**, 11 681 (1992).

[15] M.T. Hutchings and E.J. Samuelsen, Solid State Commun. **9**, 1011 (1971).